nature neuroscience

TGF-β signaling regulates neuronal C1q expression and developmental synaptic refinement

Allison R Bialas[1,2] & Beth Stevens[1,2]

Immune molecules, including complement proteins C1q and C3, have emerged as critical mediators of synaptic refinement and plasticity. Complement localizes to synapses and refines the developing visual system through C3-dependent microglial phagocytosis of synapses. Retinal ganglion cells (RGCs) express C1q, the initiating protein of the classical complement cascade, during retinogeniculate refinement; however, the signals controlling C1q expression and function remain elusive. Previous work implicated an astrocyte-derived factor in regulating neuronal C1q expression. Here we identify retinal transforming growth factor (TGF)-β as a key regulator of neuronal C1q expression and synaptic pruning in the developing visual system. Mice lacking TGF-β receptor II (TGFβRII) in retinal neurons had reduced C1q expression in RGCs and reduced synaptic localization of complement, and phenocopied refinement defects observed in complement-deficient mice, including reduced eye-specific segregation and microglial engulfment of RGC inputs. These data implicate TGF-β in regulating neuronal C1q expression to initiate complement- and microglia-mediated synaptic pruning.

Increasing evidence implicates immune molecules in synapse development and refinement. Several molecules best known for their functions in the immune system, including MHC class I (ref. 1), neuronal pentraxins[2] and complement[3], mediate synaptic remodeling in the developing mouse brain, yet surprisingly little is known about the signals regulating the expression and function of these immune molecules at developing synapses.

Classical complement cascade proteins are components of the innate immune system that mediate developmental synaptic pruning, a process critical for the establishment of precise synaptic circuits. Complement proteins C1q and C3 are expressed in the postnatal brain and localize to subsets of synapses during synaptic remodeling in the mouse retinogeniculate system[3]—a classic model for studying developmental synapse elimination. Early in postnatal development, RGCs form transient functional synaptic connections with relay neurons in the dorsal lateral geniculate nucleus (dLGN). Before eye opening around postnatal day (P) 14, many of these transient retinogeniculate synapses are eliminated while the remaining synaptic arbors are elaborated and strengthened[4–6]. *C1qa*$^{-/-}$ and *C3*$^{-/-}$ mice exhibit sustained defects in synaptic refinement and elimination, as shown by the failure to segregate into eye-specific territories and the retention of multi-innervated dLGN relay neurons[3]. However, the signals regulating complement-mediated pruning during development remain poorly understood.

As the initiator of the classical complement cascade, C1q is a critical point of regulation in this pathway. C1q, a large secreted protein composed of C1qA, C1qB and C1qC peptide chains, is the recognition domain of the initiating protein, C1, in the classical complement cascade. In the immune system, binding of C1q to apoptotic cell membranes or pathogens triggers a proteolytic cascade of downstream complement proteins, resulting in C3 opsonization and phagocytosis by macrophages that express complement receptors. The function of complement proteins in the brain appears analogous to their immune system function: clearance of cellular material that has been 'tagged' for elimination. Consistent with the well-ascribed role of complement proteins as opsonins, or "eat me" signals, C1q and C3 localize to retinogeniculate synapses, and presynaptic terminals of retinal ganglion cells are similarly eliminated by phagocytic microglia expressing complement receptors. Genetic elimination of C1q, C3 or the microglia-specific complement receptor, CR3 (CD11b), results in sustained defects in eye-specific segregation[7], suggesting that these molecules function in a common pathway to refine synaptic circuits[3,7]. Notably, microglial engulfment of retinogeniculate inputs occurs during the narrow window of postnatal development (P5–P8) coincident with retinal C1q expression[3], suggesting that complement-dependent synaptic pruning may be initiated by C1q in the developing brain.

Remarkably little is known about the signals controlling C1q expression and function in the brain. In contrast to microglia, which express C1q continuously throughout development, RGCs express C1q in a developmentally restricted manner peaking during the early postnatal period when RGC axons undergo synaptic pruning[3]. Given the developmental expression of C1q in RGC neurons, we posited that RGC-derived C1q may be key in refinement of RGC synapses onto their target neurons in the dLGN. We therefore sought to identify the signals regulating C1q expression in RGCs and to determine whether retinal C1q is required to initiate downstream complement-dependent synaptic refinement and microglia-mediated synaptic pruning in the dLGN.

A screen investigating how astrocytes influence neuronal gene expression first identified the *C1q* genes among the few that were

[1]Department of Neurology, F.M. Kirby Neurobiology Center, Boston Children's Hospital, Harvard Medical School, Boston, Massachusetts, USA. [2]Program in Neuroscience, Harvard Medical School, Boston, Massachusetts, USA. Correspondence should be addressed to B.S. (beth.stevens@childrens.harvard.edu).

Received 2 June; accepted 30 September; published online 27 October 2013; doi:10.1038/nn.3560

highly upregulated in developing RGCs in response to astrocytes[3]. The presence of immature astrocytes in the retina corresponds to C1q expression in RGCs *in vivo*, suggesting that the astrocyte-derived factor that upregulates C1q in RGC cultures also regulates postnatal C1q expression in RGCs *in vivo*. Each of the three C1q genes (*C1qa*, *C1qb* and *C1qc*) were found to be highly upregulated in purified RGCs upon exposure to a feeder layer of astrocytes[3], implicating a secreted factor; however, the astrocyte-derived signal(s) that regulate C1q expression has not been identified. In the immune system, expression of complement and other immune genes can be modulated by rapid cytokine signaling pathways that regulate the inflammatory response. In the developing brain, astrocytes are a major source of cytokines, several of which potently regulate synapse development and function[8–11].

Here we identify transforming growth factor-β (TGF-β) as the factor secreted by astrocytes necessary and sufficient for C1q expression in purified RGCs. TGF-β ligands are expressed in the retina during the refinement period, and TGF-β receptors (TGFβRII) are developmentally expressed in the postnatal RGCs *in vivo*. Blocking TGF-β signaling in retinal neurons reduced C1q expression in postnatal RGCs and decreased synaptic localization of complement in the dLGN *in vivo*. Moreover, specific disruption of TGFβRII in retinal neurons inhibited complement- and microglia-mediated synaptic pruning in the dLGN, suggesting that TGF-β-dependent regulation of neuronal C1q in the retina regulates downstream complement-dependent synapse elimination in the dLGN. Taken together, our data reveal a role for the TGF-β cytokine signaling pathway in regulating C1q expression in neurons and in initiating complement-dependent synaptic refinement in the developing CNS.

RESULTS

C1q upregulation by a secreted factor is rapid and direct

Previous findings suggested that an astrocyte-derived factor triggers neuronal C1q expression[3]. In agreement with previous findings, we found that purified RGC neurons significantly upregulated the expression of the C1q genes (*C1qa*, *C1qb* and *C1qc*) upon chronic exposure (6 d) to cortical astrocytes grown on tissue culture inserts suspended above cultured RGCs (**Fig. 1a**). To determine whether C1q upregulation in RGCs was dependent on indirect, bidirectional signaling between astrocytes and neurons, we measured *C1qb* mRNA levels in purified P8 RGC cultures treated for 6 days *in vitro* (DIV) with conditioned medium collected from cortical astrocytes (ACM). Treating RGCs with ACM or astrocyte inserts resulted in a comparable 10–20 fold upregulation of C1q in RGCs (**Fig. 1a**), suggesting that an astrocyte-secreted factor directly upregulates neuronal C1q expression. Moreover, ACM collected from purified P8 retinal astrocyte cultures[12] stimulated a similar upregulation compared to purified or standard cortical astrocytes (**Fig. 1a**), suggesting that the astrocyte-derived factor that upregulates C1q in RGC cultures may also regulate C1q expression in RGCs *in vivo*.

Our results support a direct astrocyte-to-neuron signaling pathway in C1q upregulation; however, chronic exposure to astrocytes promotes many developmental changes in neurons, including robust increases in synapse number and neuronal activity[9,13]. To determine the time course for C1q upregulation, we measured *C1qa*, *C1qb* and *C1qc* mRNAs by quantitative PCR (qPCR) after ACM treatment (15 min–3 d). Surprisingly, RGCs upregulated C1q after only 15 min of ACM treatment, further supporting the idea that ACM directly triggers C1q upregulation (**Fig. 1b**). Moreover, RGCs rapidly upregulated mRNAs for *C1ra* and *C1s*, encoding the enzymes that associate with C1q to initiate the complement cascade (**Supplementary Fig. 1a**). This rapid upregulation occurred only in neurons and not in microglia or astrocytes treated with ACM for 15 min, suggesting differential regulatory mechanisms in neurons and glia (**Fig. 1c**). *C1qb* upregulation was blocked by actinomycin, a transcriptional inhibitor, confirming that this effect was a result of transcription

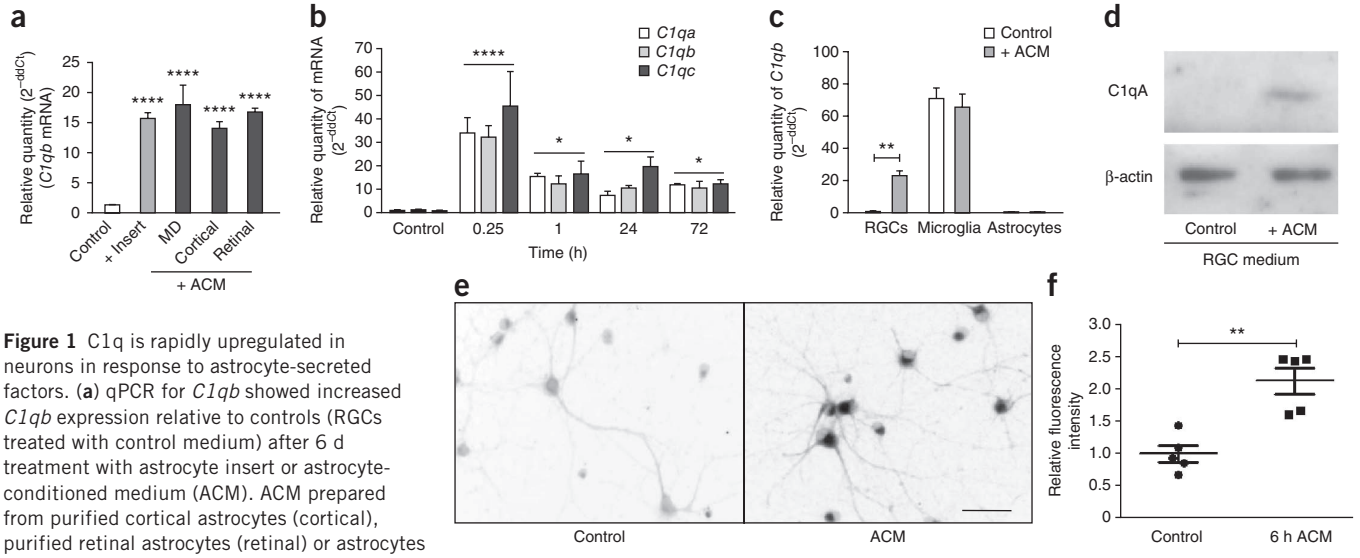

Figure 1 C1q is rapidly upregulated in neurons in response to astrocyte-secreted factors. (**a**) qPCR for *C1qb* showed increased *C1qb* expression relative to controls (RGCs treated with control medium) after 6 d treatment with astrocyte insert or astrocyte-conditioned medium (ACM). ACM prepared from purified cortical astrocytes (cortical), purified retinal astrocytes (retinal) or astrocytes prepared using the McCarthy and Devellis protocol[43] (MD) all showed a similar upregulation (one-way ANOVA, $n = 3$ experiments, $^{****}P < 0.0001$, $F_{5,12} = 75.41$). (**b**) *C1q* upregulation time course for all three *C1q* genes (*C1qa*, *C1qb* and *C1qc*) (two-way ANOVA, $n = 4$ experiments, $^{***}P < 0.001$, $^{*}P < 0.05$, $F_{4,75} = 34.37$). (**c**) qPCR results for *C1qb* showed increased *C1qb* expression relative to control in RGC cultures but not in microglia or astrocyte cultures after treatment with ACM for 15 min (two-way ANOVA, $n = 3$ experiments, $^{**}P < 0.005$, $F_{2,18} = 5.71$). (**d**) Western blot showed an increase in C1q protein in RGC medium after 6 d of treatment with ACM. Results shown are representative of 3 experiments. Full-length blots are displayed in **Supplementary Figure 6**. (**e**) There is a corresponding increase in C1q protein within 6 h of adding ACM to cultures detected by immunohistochemistry (rabbit anti-mouse C1qA[14]). Scale bar, 100 μm. (**f**) Quantification showed increased C1q in ACM-treated cultures measured as a change in fluorescence intensity relative to that of control untreated cultures (*t*-test, $n = 3$ experiments, $^{**}P < 0.01$, $t_4 = 37.48$). Error bars, s.e.m.

(**Supplementary Fig. 1b**). Furthermore, boiling ACM destroyed its ability to induce *C1qb* upregulation, implicating a protein in ACM in neuronal C1q upregulation (**Supplementary Fig. 1c**).

In addition to the upregulation of *C1qa*, *C1qb* and *C1qc* mRNAs, we observed a corresponding increase in C1qA protein as measured by western blot analysis of medium from cultures treated for 1 week with ACM (**Fig. 1d**) and by immunocytochemistry for C1q (rabbit anti-C1qA[14]) in purified RGC cultures treated with ACM (6 h) (**Fig. 1e**,**f**). ACM itself or medium from RGCs treated with ACM acutely showed undetectable C1q by western blot (data not shown), indicating that C1q produced by RGCs accumulates in the medium over time in response to ACM. Thus, we used this purified culture system as a robust assay to screen for secreted signals that rapidly upregulate and sustain C1q expression in RGCs.

TGF-β is necessary and sufficient for C1q upregulation

To identify the astrocyte-derived factor responsible for C1q upregulation, we screened several candidate molecules for the ability to upregulate C1q in purified RGC neuronal cultures. Cytokines, potent modulators of immune and neural function, were the main class of molecule we tested because astrocytes are a major source of cytokines in the brain and several cytokines elicit systemic increases in C1q in the bloodstream. We first measured several candidate cytokines in ACM by ELISA (MSD mouse 7-plex inflammatory cytokine assay and individual ELISAs for TGF-β1, TGF-β2 and TGF-β3) (**Fig. 2a**). Several cytokines were detected in ACM, including CXCL1, interleukin (IL)-12, TGF-β1, TGF-β2 and TGF-β3. To determine which cytokines were required for astrocyte-dependent C1q upregulation in RGC neurons, we immunodepleted individual cytokines from ACM. Two of the cytokines most enriched in ACM, CXCL1 and IL-12, showed no effect on *C1qb* expression when added to cultures as recombinant protein (**Supplementary Fig. 1d**,**e**); thus, we did not perform immunodepletion of these cytokines. Although tumor necrosis factor-α and IL-6 induced modest *C1qb* upregulation when added directly to RGC cultures (**Supplementary Fig. 1f**), immunodepletion of these cytokines did not affect ACM-induced *C1qb* upregulation (**Fig. 2b**). In contrast, specific immunodepletion of TGF-β from ACM using an anti–pan-TGF-β neutralizing antibody (1D11, R&D Systems) prevented ACM-induced *C1qb* upregulation after 15 min of treatment, as measured by qPCR (**Fig. 2b**). We verified TGF-β immunodepletion from ACM by ELISA (**Fig. 2c**). Together, these data show that TGF-β is necessary to upregulate neuronal C1q in purified RGC cultures.

To determine which TGF-β isoform was upregulating *C1q* expression, we depleted individual TGF-β isoforms from ACM using antibodies specific to TGF-β1, TGF-β2 or TGF-β3 (R&D Systems). Only ACM depleted of TGF-β3 failed to upregulate *C1qb* in RGCs, suggesting that this isoform may be key in regulating

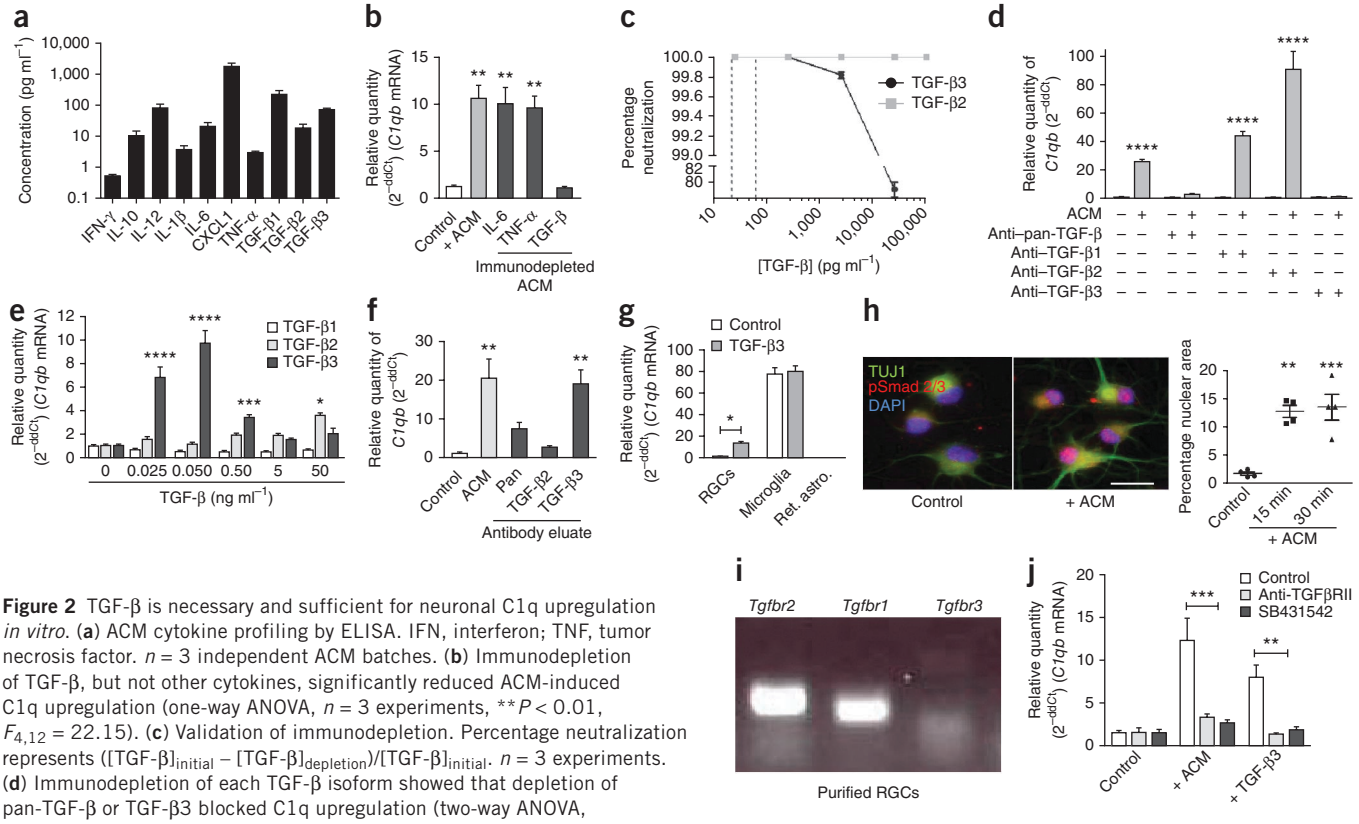

Figure 2 TGF-β is necessary and sufficient for neuronal C1q upregulation *in vitro*. (**a**) ACM cytokine profiling by ELISA. IFN, interferon; TNF, tumor necrosis factor. $n = 3$ independent ACM batches. (**b**) Immunodepletion of TGF-β, but not other cytokines, significantly reduced ACM-induced C1q upregulation (one-way ANOVA, $n = 3$ experiments, $^{**}P < 0.01$, $F_{4,12} = 22.15$). (**c**) Validation of immunodepletion. Percentage neutralization represents $([\text{TGF-}\beta]_{\text{initial}} - [\text{TGF-}\beta]_{\text{depletion}})/[\text{TGF-}\beta]_{\text{initial}}$. $n = 3$ experiments. (**d**) Immunodepletion of each TGF-β isoform showed that depletion of pan-TGF-β or TGF-β3 blocked C1q upregulation (two-way ANOVA, $n = 3$ experiments, $^{****}P < 0.0001$, $F_{4,20} = 79.52$). (**e**) Concentration-response curves for TGF-β1, TGF-β2 and TGF-β3 (two-way ANOVA, $n = 3$ experiments, $^{****}P < 0.0001$, $^{***}P < 0.001$, $^{*}P < 0.05$, $F_{10,36} = 23.56$). (**f**) Glycine elution showed that either anti–pan-TGF-β (Pan) or anti–TGF-β3 eluates upregulate C1q (one-way ANOVA, $n = 3$ experiments, $^{**}P < 0.01$, $F_{4,10} = 11.02$). (**g**) qPCR results for *C1qb* in RGC cultures and in microglia or retinal astrocyte (ret. astro.) cultures after TGF-β3 treatment (50 pg ml^{-1}) for 15 min (two-way ANOVA, $n = 3$ experiments, $^{*}P < 0.05$, $F_{2,12} = 415.96$). (**h**) RGCs showed increased nuclear accumulation of pSmad2 (15–30 min ACM treatment). Quantification showed a significant increase in pSmad (red) within the nuclear area (blue) (one-way ANOVA, $n = 15$ cells per condition, $^{***}P < 0.001$, $^{**}P < 0.01$, $F_{2,9} = 19.83$). Scale bar, 20 μm. (**i**) RT-PCR for *Tgfbr1*, *Tgfbr2* and *Tgfbr3* in P5 retina. Data shown are representative of 4 samples tested. Full-length gels are displayed in **Supplementary Figure 6**. (**j**) Blocking TGFβRII signaling with neutralizing antibodies or with inhibitors of TGFβRI significantly reduced the effects of ACM or TGF-β3 (50 pg ml^{-1}) on C1q (two-way ANOVA, $n = 3$ experiments, $^{**}P < 0.01$, $^{***}P < 0.001$, $F_{4,18} = 35.06$). Error bars, s.e.m.

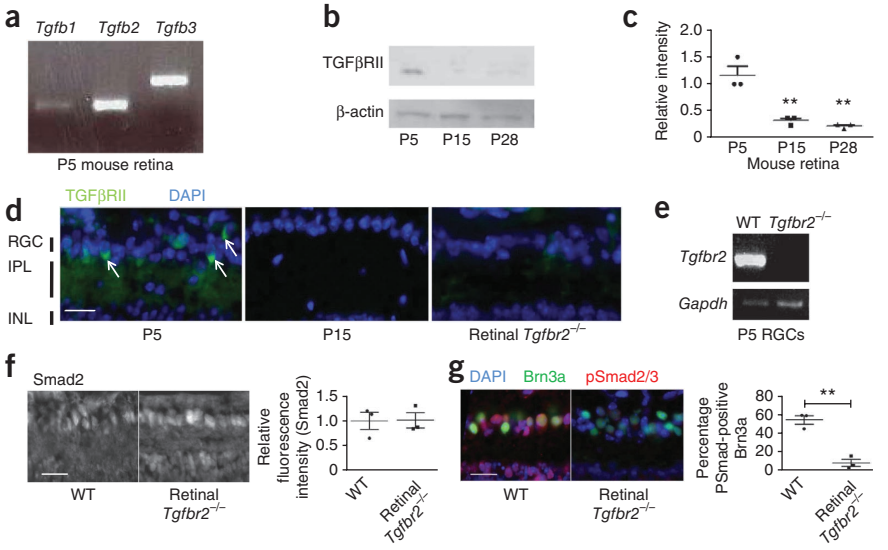

Figure 3 TGF-β expression corresponds to synaptic refinement period in the retinogeniculate system. (**a**) RT-PCR showed expression of all three *Tgfb* isoforms in the P5 mouse retina. Data are representative of 4 mice. (**b**) Western blot for TGFβRII (goat anti-human TGFβRII, R&D Systems) showed developmental expression of TGFβRII in the mouse retina. See **Supplementary Figure 6** for full-length blot. (**c**) Relative intensity quantification normalized to β-actin control for each age showed developmental TGFβRII expression in the postnatal mouse retina (one-way ANOVA, $n = 3$ experiments, $^{**}P < 0.01$, $F_{2,6} = 26.36$). (**d**) Immunostaining with antibodies against TGFβRII (R&D Systems, goat anti-TGFβRII) showed that the receptor localizes to the RGC layer and the IPL (arrows) and that staining intensity is reduced at P15 relative to P5. Antibody staining was confirmed for specificity by staining retinal *Tgfbr2*$^{-/-}$ mice. All images were obtained with equal exposure times. Scale bar, 50 μm. (**e**) RT-PCR confirmed the absence of *Tgfbr2* mRNA in RGCs acutely isolated from retinal *Tgfbr2*$^{-/-}$ P5 mice using immunopanning. Data shown are representative of 4 animals tested. Full-length gel in **Supplementary Figure 6**. (**f**) Immunohistochemistry for total Smad2 showed no difference in relative fluorescence intensity (RGC layer) in WT littermates and retinal *Tgfbr2*$^{-/-}$ mice (*t*-test, $n = 3$ mice per genotype, $P = 0.96$, $t_4 = 0.053$). Scale bar, 50 μm. (**g**) Immunohistochemistry for pSmad. Co-staining for an RGC marker, Brn3a, and pSmad2/3 showed a significant reduction in pSmad in RGCs specifically (*t*-test, $n = 3$ mice per group, $^{**}P < 0.01$, $t_4 = 13.18$). Scale bar, 50 μm. Error bars, s.e.m.

neuronal C1q (**Fig. 2d**). Furthermore, we generated concentration-response curves (25 pg ml^{-1}–50 ng ml^{-1}) in RGC cultures for each of the TGF-β isoforms and measured *C1qb* expression by qPCR. TGF-β3 most effectively upregulated *C1qb* in RGCs at concentrations similar to those measured in ACM, whereas TGF-β2 modestly upregulated *C1qb* at high concentrations (**Fig. 2e**). In addition, glycine elution to release ACM-derived bound TGF-β from anti–pan-TGF-β or anti–TGF-β3 neutralizing antibodies produced an eluate that could upregulate *C1qb* to the same extent as ACM when added to RGC cultures (**Fig. 2f**). We also found that retinal astrocytes showed enrichment for TGF-β3 when compared with RGCs, cortical astrocytes and microglia (**Supplementary Fig. 1g**). However, treating retinal astrocyte or microglial cultures with recombinant TGF-β3 (50 pg ml^{-1}, 15 min) failed to induce *C1qb* upregulation (**Fig. 2g**), in agreement with our findings with ACM treatment (**Fig. 1c**). Taken together, these results demonstrate that, of the cytokines tested, TGF-β is a major component in ACM responsible for C1q upregulation in RGCs but not in microglia or astrocytes (**Fig. 2g**). Furthermore, our findings suggest that TGF-β3 may be the key isoform regulating C1q expression in RGCs (**Fig. 2d**,**f**).

We next addressed whether TGF-β receptor signaling in RGCs is required for C1q upregulation in RGCs. In the canonical TGF-β signaling pathway, TGF-β1, TGF-β2 or TGF-β3 binds to TGFβRII, which then phosphorylates TGFβRI. Once activated, TGFβRI phosphorylates a Smad transcription factor to alter gene expression. A third receptor, TGFβRIII, can also associate with TGFβRII, and it alters ligand affinity[15]. Purified RGCs express all of the components required for TGF-β signaling (**Fig. 2h**,**i**). Furthermore, treating RGCs with ACM stimulated rapid (15–30 min) nuclear accumulation of phosphorylated Smads 2 and/or 3 (pSmad2/3), as measured by immunocytochemistry (**Fig. 2h**), which is consistent with the timing of C1q upregulation. In addition, transcripts for TGFβRII, TGFβRIII and TGFβRI were present in purified RGCs (**Fig. 2i**). These data indicate that RGCs express functional TGF-β receptors that can be activated with a time course consistent with that of C1q upregulation.

To determine whether the TGF-β receptors TGF-βRI and TGF-βRII were responsible for this upregulation, we preincubated RGC cultures with specific inhibitors of TGFβRI and TGFβRII before acute treatment with either TGF-β3 (50 pg ml^{-1}) or ACM. Adding TGFβRII neutralizing antibodies (R&D Systems) or a TGFβRI-specific inhibitor[16] (SB431542, Tocris, 30 μM) blocked both TGF-β-induced and ACM-induced C1q upregulation (**Fig. 2j**). Thus, signaling through TGFβRI and TGFβRII is required for ACM-induced C1q upregulation in purified RGCs.

TGF-β regulates developmental C1q expression in the retina

C1q is developmentally regulated in the postnatal retina, showing peak expression around P5 and sharply decreasing by P10–P15 (ref. 3), corresponding to the synaptic refinement period in the retinogeniculate system and the presence of immature astrocytes throughout the developing CNS (**Supplementary Fig. 2a**). To determine whether TGF-β signaling regulates developmental C1q expression in RGCs *in vivo*, we examined the expression of TGF-β signaling components during the refinement period. We detected expression of all three isoforms of *Tgfb* by reverse transcription (RT)-PCR at P5 and in the mature retina (**Fig. 3a**). In addition, we detected TGFβRII protein in retinal lysates by western blot (**Fig. 3b**). Of the three ages examined, the level of TGFβRII protein was highest at P5 and sharply decreased by P15 and P28 (**Fig. 3b**,**c**), coinciding with C1q expression in the postnatal retina (**Supplementary Fig. 2a**). In agreement with western blot analysis, immunohistochemistry for TGFβRII showed TGFβRII localization to the RGC and inner plexiform layers (IPL) of the retina at P5 and a decrease in TGFβRII by P15 (**Fig. 3d**). Co-staining with anti-calretinin (Millipore), a marker of a subset of RGCs, confirmed TGFβRII localization to RGCs (**Supplementary Fig. 2b**). Taken together, these data show that TGF-β ligands and receptors are present at the right time in the retina to regulate C1q expression.

To determine whether TGF-β signaling regulates C1q expression *in vivo* during retinogeniculate refinement, we used genetic and pharmacological approaches to block TGF-β signaling and then measured C1q expression *in vivo*. Retina-specific *Tgfbr2*$^{-/-}$ mice were generated

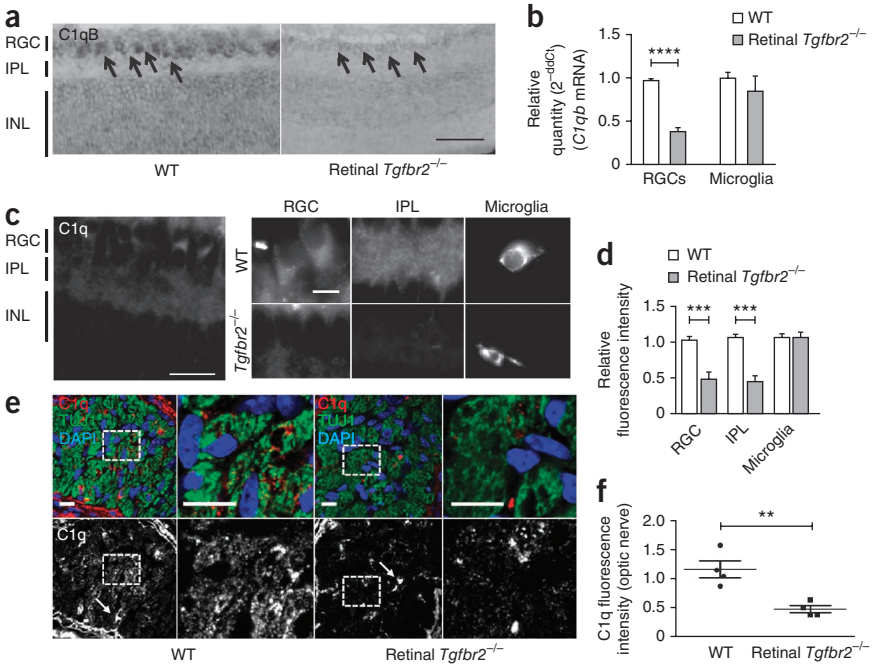

Figure 4 TGF-β signaling is required for neuronal C1q expression *in vivo*. (**a**) *In situ* hybridization for *C1qb* showed significantly reduced expression in the RGC layer (arrows) in retinal *Tgfbr2*$^{-/-}$ mice. Scale bar, 100 µm. (**b**) RGCs acutely isolated from P5 retinal *Tgfbr2*$^{-/-}$ retinas using immunopanning showed significantly reduced *C1qb* expression as compared to WT. Microglia acutely isolated using CD45 immunopanning showed no significant difference in *C1qb* levels (two-way ANOVA, $n = 5$ mice per group, $^{****}P < 0.0001$, $F_{1,16} = 19.11$). (**c**) Immunostaining for C1q in P5 retina (scale bars: left, 50 µm; right, 20 µm). In retinal *Tgfbr2*$^{-/-}$ mice, C1q localization to the RGC layer and the IPL was reduced relative to that in WT animals. Retinal microglia showed no change in C1q levels. (**d**) Quantification of the relative fluorescence intensity in each retinal area in WT littermates and retinal *Tgfbr2*$^{-/-}$ mice. C1q localization to the RGC layer and IPL was significantly reduced when TGF-β signaling was blocked (two-way ANOVA, $n = 4$ mice per group, $^{***}P < 0.001$, $F_{2,12} = 11.69$). (**e**) Immunohistochemistry for C1q in optic nerve cross sections showed C1q-immunopositive puncta co-localized with RGC axon fascicles labeled by TUJ1 (green). C1q levels were significantly reduced in the retinal *Tgfbr2*$^{-/-}$ mouse within the axon, as indicated by co-localization with TUJ1. C1q labeling of microglia remained unchanged (arrows). Scale bars, 10 µm. (**f**) Quantification of the fluorescence intensity for C1q staining with axon bundles shows a significant decrease in C1q (*t*-test, $n = 3$ mice (two nerves per mouse), $^{**}P = 0.0055$, $t_6 = 4.225$). Error bars, s.e.m.

by crossing mice with a *loxP*-flanked *Tgfbr2* gene with mice expressing Cre recombinase under the control of the mouse *Chx10* (also known as *Vsx2*) promoter, which is active at embryonic day 13.5 in the outer neuroblastic layer of the retina only[17,18]. TGFβRII knockout was confirmed by immunostaining retinas (**Fig. 3d**) and performing RT-PCR using mRNA from wild-type (WT) and transgenic P5 whole brain (**Supplementary Fig. 2c**) and purified RGCs acutely isolated from P5 WT and transgenic mice (**Fig. 3e**). Klf10 (*Tieg*), whose expression is known to be TGF-β dependent, also showed reduced expression in P5 acutely isolated RGCs (**Supplementary Fig. 2d**). Moreover, while total Smad2 levels were not significantly different between WT and retinal *Tgfbr2*$^{-/-}$ mice (**Fig. 3f**), pSmad2/3 levels, corresponding to active TGF-β signaling, were reduced in RGCs identified by co-staining with Brn3a, a POU-domain transcription factor specific to this cell type (**Fig. 3g**), further indicating that TGFβRII retina-specific knockout was achieved. Because TGF-β signaling has many roles in development, we measured cell numbers, axon density and axon caliber and found no significant difference from WT retinas (**Supplementary Fig. 2e–h**). Given that there were no gross abnormalities in retinal development, we used this mouse to analyze the role of TGF-β signaling in C1q regulation and synaptic refinement.

To determine whether retinal TGF-β signaling is required for developmental C1q expression in RGCs, we assayed C1q expression levels in retinas and RGCs from retinal *Tgfbr2*$^{-/-}$ mice relative to those in WT littermates and from mice receiving intravitreal injection of anti–TGF-β relative to those in vehicle-treated littermates. *In situ* hybridization for *C1qb* revealed a decrease in signal for *C1qb* in the RGC layer in retinal *Tgfbr2*$^{-/-}$ retinas (P5) compared to that in WT littermates (**Fig. 4a**; anti–TGF-β, **Supplementary Fig. 3a**). To verify that reduction in C1q expression was in RGCs and not other cell types in the RGC layer, we acutely isolated RGCs and microglia from P5 retinas using established immunopanning techniques[12,19]. Acutely isolated RGCs from the retinal *Tgfbr2*$^{-/-}$ mice showed a significant reduction in *C1qb* expression by qPCR, whereas acutely isolated retinal microglia did not (**Fig. 4b**), as expected given that microglia do not express *Chx10*. Similarly, RGCs acutely isolated from P5 mice receiving intravitreal injection at P3 of anti–TGF-β also showed significantly reduced *C1qb* expression, whereas microglia again showed no change in C1q (two-way ANOVA, $n = 4$ mice per group, $P < 0.05$, $F_{2,18} = 7.108$; **Supplementary Fig. 3b**). We verified cell purity after immunopanning using qPCR for the neuron-specific mRNA *Eno2* (*Nse*) and the microglia-specific mRNA *Iba1* (**Supplementary Fig. 3c**). Moreover, immunohistochemistry for C1q at P5 in retinal *Tgfbr2*$^{-/-}$ (**Fig. 4c**,**d**) and anti–TGF-β–injected mice (**Supplementary Fig. 3d**,**e**) also showed a 40–50% reduction in C1q immunostaining in the IPL and RGC layers of the retina but showed no change in microglial staining. Taken together, these data show that TGF-β signaling is required for postnatal C1q expression in RGCs. These results also suggest that TGF-β regulation of C1q may be restricted to neurons, as suggested by our earlier *in vitro* data (**Fig. 1c**).

Retinal TGF-β regulates complement levels in the thalamus

C1q and C3 localize to synapses in the dLGN during the period of synaptic refinement, but whether RGC neurons are a key source of C1q in the dLGN is not known. One possibility is that neuronal C1q is locally secreted from RGC axons into the dLGN to initiate complement-dependent synaptic pruning. Alternatively, microglia, although sparse in the dLGN at this time, may be a primary source of secreted C1q in the postnatal dLGN during refinement. To address this question, we examined C1q protein levels by immunohistochemistry in cross-sections of P5 optic nerve. C1q could be detected in optic nerve fiber bundles, identified by TUJ1 staining. Moreover, C1q immunoreactivity in the optic nerve was significantly reduced in

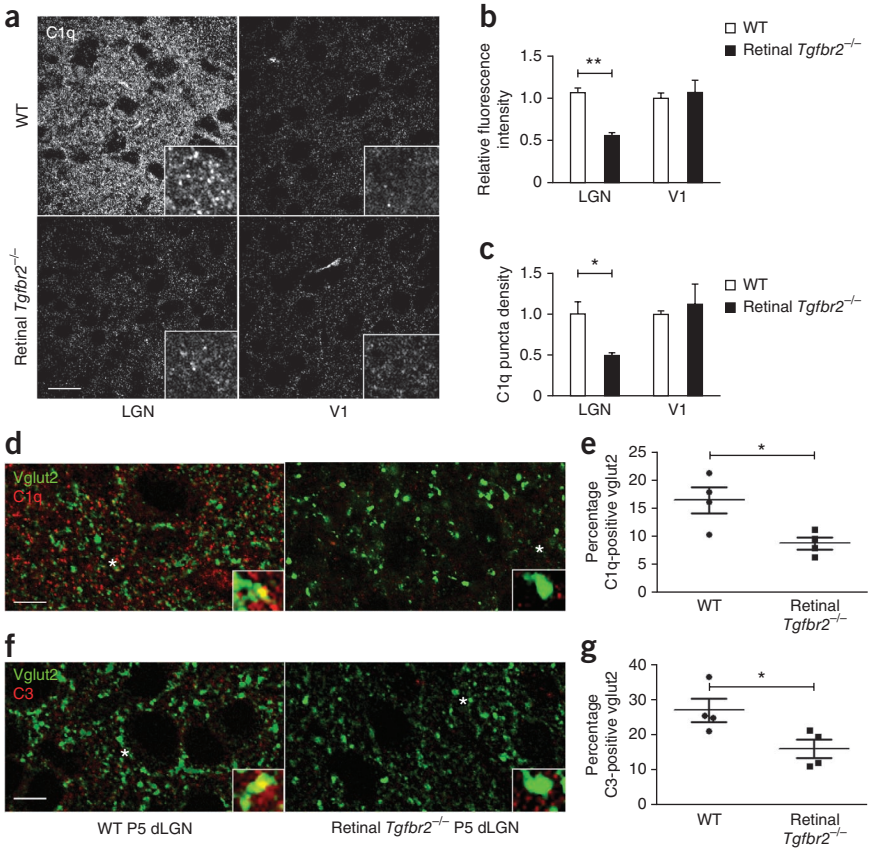

Figure 5 Retinal TGF-β signaling is required for complement localization in the dLGN. (**a**) C1q immunohistochemistry in the dLGN and V1 shows reduced C1q fluorescence in the dLGN but not in V1. Scale bar, 20 µm. Insets show 3× magnification. (**b**) Quantifying relative fluorescence intensity showed significant reduced intensity in the dLGN of retinal *Tgfbr2*$^{-/-}$ versus WT mice (two-way ANOVA, $n = 4$ mice per group, $^{**}P < 0.01$, $F_{1,12} = 11.21$). No differences were observed in V1. (**c**) Quantification showed significantly reduced density of C1q puncta in the dLGN in retinal *Tgfbr2*$^{-/-}$ mice versus WT littermates (two-way ANOVA, $n = 4$ mice per group, $^{*}P < 0.05$, $F_{1,8} = 7.48$). No difference in C1q puncta density was observed in V1. (**d**) Immunostaining for C1q and vglut2 in WT and retinal *Tgfbr2*$^{-/-}$ P5 dLGNs showed a reduction in colocalization of C1q and vglut2. Scale bar, 20 µm. White asterisks indicate the synaptic puncta enlarged 3.5× in the inset. (**e**) Quantification of C1q co-localization with vglut2 showed significantly reduced synaptic localization of C1q in retinal *Tgfbr2*$^{-/-}$ mice (*t*-test, $n = 4$ mice, $^{*}P = 0.0226$, $t_6 = 3.045$). (**f**) Immunostaining for C3 and vglut2 in WT and retinal *Tgfbr2*$^{-/-}$ P5 dLGNs. C3 localization to vglut2-positive RGC terminals is reduced in the retinal *Tgfbr2*$^{-/-}$ mice, as observed for C1q. Scale bar, 20 µm. (**g**) Co-localized C3 and vglut2 puncta were identified and counted using ImageJ Puncta Analyzer (*t*-test, $n = 4$ mice, $^{*}P = 0.0395$, $t_6 = 2.622$). Error bars, s.e.m.

retinal *Tgfbr2*$^{-/-}$ mice versus WT littermates (**Fig. 4e**,**f**), suggesting that TGF-β signaling in RGCs regulates C1q in RGC axons in the optic nerve.

If C1q in the dLGN is supplied by RGCs, we predicted that retinal *Tgfbr2*$^{-/-}$ mice would have a reduction in C1q protein throughout the dLGN. Indeed, immunohistochemistry for C1q revealed a significant decrease in the intensity of C1q staining in the dLGN but not in primary visual cortex (V1) (**Fig. 5a**), which is not a direct target for RGCs. Quantification showed a significant reduction in fluorescence intensity in the retinal *Tgfbr2*$^{-/-}$ mice, as well as a significant decrease in the density of C1q puncta in the dLGN but not in V1 (**Fig. 5b**,**c**), indicating that RGC axons are a key source of C1q in the postnatal dLGN.

Given previous findings that C1q and C3 localize to synapses in the dLGN, we examined synaptic localization of complement in the dLGN in retinal *Tgfbr2*$^{-/-}$ mice and WT littermates to determine whether synaptic localization of these proteins depends on retinal TGF-β signaling. Immunostaining in the dLGN using antibodies to C1q, C3 and vesicular glutamate transporter 2 (vglut2) to label RGC terminals showed approximately 15% of vglut2-positive puncta co-labeled with C1q (**Fig. 5d**,**e**) and ~25% of vglut2 puncta co-stained with the downstream complement protein, C3 (**Fig. 5f**,**g**). The increase in the number of RGC terminals labeled with C3 versus C1q is consistent with the placement of these molecules in the classical complement cascade, as multiple C3 molecules can be activated downstream of a single C1q molecule. Also, as expected given that C1q is upstream of C3 activation in the complement cascade, we found that C3 deposition in the dLGN was undetectable in the *C1q*$^{-/-}$ mouse (**Supplementary Fig. 3f**). In retinal *Tgfbr2*$^{-/-}$ dLGNs, we also observed a significant reduction in synaptic localization of both C1q and C3 (**Fig. 5d–g**).

Given that retinal *Tgfbr2*$^{-/-}$ exhibit specific reduction in TGF-β signaling and C1q in the retina, a reduction in C1q and C3 synaptic localization in the dLGN suggests that an appreciable fraction of synaptically localized C1q is supplied by RGC terminals and that C1q and C3 localization to synapses is dependent on retinal TGF-β signaling. Thus, local microglia-derived C1q in the dLGN does not appear to localize to synapses to compensate for the loss of RGC-derived C1q.

TGF-β signaling is required for eye-specific segregation

In *C1qa*$^{-/-}$ mice, RGC axons do not segregate into eye-specific territories normally as assessed by anterograde tracing techniques[3]. If C1q supplied by RGC axons is required for eye-specific segregation and if retinal TGF-β signaling regulates C1q expression, then retinal *Tgfbr2*$^{-/-}$ mice should exhibit a phenotype similar to that of *C1qa*$^{-/-}$ mice. To test this hypothesis, we used established anterograde tracing techniques to visualize the formation of eye-specific territories in the dLGN and to assay eye-specific segregation in retinal *Tgfbr2*$^{-/-}$ mice and in mice injected with anti–TGF-β. Mice received intraocular injections of cholera toxin-β conjugated to Alexa 488 or Alexa 594 (CTB-488 or CTB-594) at P9 in the left and right eyes, respectively, and mice were sacrificed at P10. We assayed eye-specific segregation using an unbiased assay in which the degree of segregation is represented by the variance of the distribution of the *R* value, the logarithm of the ratio of fluorescence intensity (*F*) from each fluorescence channel (that is, $R = \log_{10}(F_{ipsi}/F_{contra})$)[20]. Using this assay, high variance signifies a high degree of segregation in the dLGN, while low variance corresponds to increased overlap between contralateral and ipsilateral territories. Our results showed a significantly lower variance in *C1qa*$^{-/-}$ mice than in WT controls, as expected (**Fig. 6a**,**b**). Notably, we observed a similar phenotype in retinal *Tgfbr2*$^{-/-}$ mice (**Fig. 6a**,**b**)

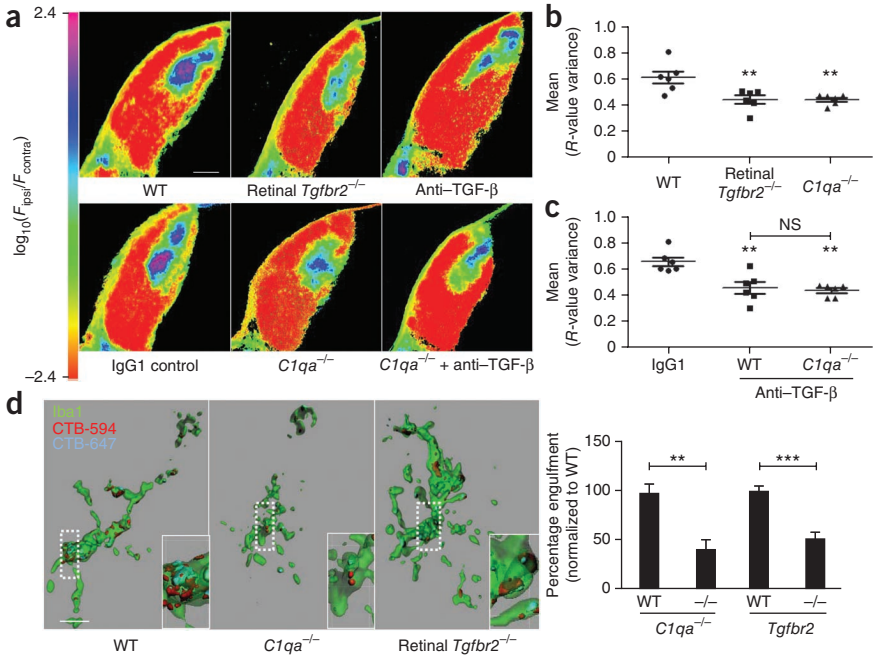

Figure 6 TGF-β signaling and C1q are required for eye-specific segregation and microglia-mediated pruning in the retinogeniculate system. (**a**) Representative dLGN images for WT, retinal *Tgfbr2*$^{-/-}$, *C1qa*$^{-/-}$, IgG1–injected controls and anti–TGF-β–injected WT and *C1qa*$^{-/-}$ mice pseudocolored to show the *R* value for each pixel. Scale bar, 100 µm. (**b**) Quantification of the mean variance of the *R* value for each group. There is a significant reduction in the mean variance of the *R* value in mice deficient in TGF-β signaling or C1q (one-way ANOVA, $n = 6$ animals per group, $^{**}P < 0.01$, $F_{2,15} = 8.228$). (**c**) There is no additional decrease in the *R*-value variance when TGF-β signaling is blocked in *C1qa*$^{-/-}$ mice (one-way ANOVA, $n = 6$ animals per group, $^{**}P < 0.01$, $F_{2,15} = 8.567$; NS, not significant ($P = 0.701$)). (**d**) Microglia show reduced engulfment of RGC terminals in mice deficient in C1q or retinal TGF-β signaling. Volume of each microglia and the engulfed CTB was quantified in Imaris and the percentage engulfment defined as the volume of internalized CTB/volume of microglia. Results were normalized to WT engulfment levels. *C1qa*$^{-/-}$ or retinal TGFβRII$^{-/-}$ mice both showed a significant reduction in percentage engulfment (one-way ANOVA, $n = 6$ mice per group, $^{***}P < 0.001$, $^{**}P < 0.01$, $F_{3,20} = 13.66$). Scale bar, 10 µm. Insets show enlargement of boxed area. Error bars, s.e.m.

and mice injected with anti–TGF-β (**Fig. 6a**,**c**), suggesting a common pathway. Defects in eye-specific segregation were confirmed by also quantifying the percentage of dLGN area innervated by both contralateral and ipsilateral RGC inputs (**Fig. 7a**,**b**). Measurement of dLGN area showed no difference between WT and retinal *Tgfbr2*$^{-/-}$ (**Fig. 7c**), and we detected no difference in dLGN relay neuron number (data not shown), determined by immunohistochemistry for unphosphorylated neurofilament (SMI-32), in retinal *Tgfbr2*$^{-/-}$ mice as compared to WT.

Our results showed that retinal TGF-β was required for eye-specific segregation, but it was not clear whether this effect occurred through regulation of C1q. To determine whether TGF-β could regulate synaptic refinement independently of C1q, we performed

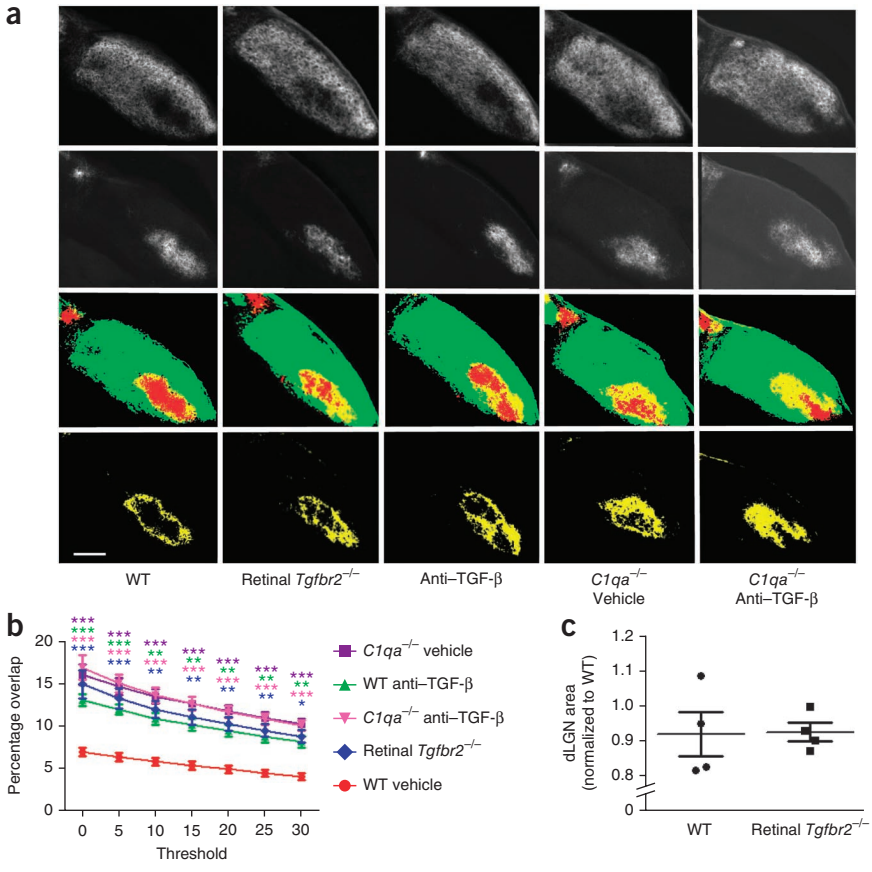

Figure 7 Mice deficient in C1q or retinal TGF-β signaling show increased overlap of contralateral and ipsilateral areas in the dLGN. (**a**) Representative images of anterograde tracing (Alexa-conjugated CTB) of contralateral (top row) and ipsilateral (second row) retinogeniculate projections, merged channels (third row) and their overlap (yellow, bottom row) in the dLGN for WT, retinal *Tgfbr2*$^{-/-}$, *C1qa*$^{-/-}$ and anti–TGF-β–injected WT and *C1qa*$^{-/-}$ mice. Scale bar, 100 µm. (**b**) Quantification of percentage of dLGN area receiving input from both contralateral and ipsilateral eyes (yellow area). Data shown as mean yellow area ± s.e.m. (two-way ANOVA, $n = 6$ animals per group, $^{***}P < 0.001$, $^{**}P < 0.01$, $^{*}P < 0.05$, $F_{4,175} = 101.00$). (**c**) Measurements of dLGN area in P10 mice showed no significant difference between WT and retinal *Tgfbr2*$^{-/-}$ mice. Results were normalized to WT dLGN area and 4 dLGNs were analyzed per mouse (*t*-test, $n = 4$ mice, $P = 0.9342$, $t_6 = 0.08611$). Error bars, s.e.m.

intraocular injection of anti–TGF-β neutralizing antibodies in WT and *C1qa*$^{-/-}$ animals to determine whether blocking TGF-β would disrupt synaptic refinement in the absence of C1q. If TGF-β and C1q regulate pruning by different mechanisms, blocking TGF-β in *C1qa*$^{-/-}$ mice should produce a more severe segregation defect, or increased overlap, than that in vehicle-injected *C1aq*$^{-/-}$ mice. If TGF-β and C1q are in the same pathway, blocking TGF-β signaling in the *C1qa*$^{-/-}$ mouse should have no effect. Blocking TGF-β in the *C1qa*$^{-/-}$ mouse did not result in a more severe phenotype, which is consistent with TGF-β exerting its effect on synaptic refinement via regulation of C1q (**Figs. 6a–c** and **7a**,**b**). Taken together, these results show that retinal TGF-β signaling is required for eye-specific segregation and that TGF-β and C1q likely work in the same pathway to regulate this process.

Retinal TGF-β and C1q regulate microglia-mediated pruning

Engulfment of retinogeniculate synapses by microglia is thought to be the final step in complement-dependent synapse elimination. Recent work has demonstrated that microglia engulf RGC terminals in the dLGN during the pruning period in a complement (C3-CR3)-dependent manner[7]. Therefore, if RGC-derived C1q regulates this process, we predict retinal *Tgfbr2*$^{-/-}$ mice to show a reduction in microglial engulfment of RGC terminals.

To test this hypothesis, we used an established microglia engulfment assay[7] to quantify microglial phagocytosis of RGC inputs in *C1qa*$^{-/-}$ mice and retinal *Tgfbr2*$^{-/-}$ mice. We found a significant reduction in microglial engulfment of RGC inputs at P5 in *C1qa*$^{-/-}$ and *Tgfbr2*$^{-/-}$ mice as compared to littermate controls (**Fig. 6d**). We found no differences in the number, distribution or activation state of microglia in the dLGN in WT versus *C1qa*$^{-/-}$ or *Tgfbr2*$^{-/-}$ conditions (**Supplementary Fig. 4a–d**). These results show that reduction of retinal TGF-β signaling, and consequently of C1q expression in RGCs, reduces microglial phagocytosis of RGC terminals in the dLGN. Together these data support the hypothesis that RGC-derived C1q is required to initiate the process of complement-dependent synapse elimination by microglia.

DISCUSSION

This study establishes that TGF-β signaling in RGC neurons plays a key role in refinement of RGC synapses on their target relay neurons in the dLGN by regulating expression of C1q, the initiating protein of the classical complement cascade. We demonstrate that TGF-β signaling is necessary and sufficient for transcriptional upregulation of C1q in purified RGCs (**Fig. 2**). In agreement with *in vitro* studies, conditional knockout of TGFβRII in retinal neurons reduced C1q expression in RGCs during the period of active refinement of retinogeniculate synapses in the thalamus (**Fig. 4**). Furthermore, our data show that C1q and C3 localization to synapses in the dLGN during retinogeniculate refinement is dependent on retinal TGF-β signaling (**Fig. 5**). Inhibition of TGF-β signaling in the postnatal retina resulted in defects in eye-specific segregation in the dLGN, mimicking the phenotype observed in global *C1qa*$^{-/-}$ mice (**Fig. 6a–c**). We also observed defects in microglial engulfment of RGC terminals (**Fig. 6d**), which phenocopied the *C3*$^{-/-}$ and *CR3*$^{-/-}$ (*Itgam*$^{-/-}$) mouse microglial engulfment defects[7]. Taken together, our findings support a model in which retinal TGF-β signaling controls C1q expression in RGCs and local C1q release in the dLGN to regulate microglia-mediated, complement-dependent synaptic refinement (**Supplementary Fig. 5**).

C1q regulates microglia-mediated pruning in the thalamus

Emerging evidence implicates microglia in developmental synaptic refinement[7,21,22]; however, the mechanisms controlling the timing and location of microglia-mediated synaptic refinement in the brain are poorly understood. Process-bearing phagocytic microglia in the postnatal dLGN engulf RGC inputs during retinogeniculate refinement in a manner dependent on complement C3-CR3 signaling and neuronal activity[7]. Upon complement cascade activation, C3 is cleaved to form the potent opsonin C3b, a ligand for the phagocytic complement receptor CR3 expressed in the brain by microglia exclusively. Thus, as the initiator of the classical complement cascade, C1q is a critical regulator of C3 activation and C3-dependent phagocytosis. Our results suggest that C3 localization to synapses (**Fig. 5**) and microglia-mediated pruning (**Fig. 6**) depend on retina-derived C1q. Specifically, we observed a decrease in C3 localization to synapses in *C1qa*$^{-/-}$ and in retinal *Tgfbr2*$^{-/-}$ mice. We also found that microglial engulfment of RGC terminals is decreased in *C1qa*$^{-/-}$ (**Fig. 6d**) and in retinal *Tgfbr2*$^{-/-}$ mice (**Fig. 6d**), placing retina-derived C1q and retinal TGF-β signaling upstream of this process.

Interestingly, recent work revealed that microglia-mediated pruning is regulated by neuronal activity[7]. During the retinogeniculate pruning period, microglia preferentially engulf less active RGC inputs in the dLGN[7], suggesting that microglia can sense or read out local changes in synaptic activity. The engulfment defects observed in complement-deficient mice and the role for complement in the immune system suggest the intriguing possibility that complement proteins could be one cue guiding microglia to engulf less active synapses. Other immune molecules implicated in synaptic refinement, such as MHC class I (ref. 23) and neural pentraxins[24], show activity-dependent transcriptional regulation, but whether these molecules influence activity-dependent microglial engulfment is unknown. Interestingly, C1q expression corresponds to the onset of spontaneous neuronal activity in the retina, and the *C1qa*$^{-/-}$ phenotype closely mimics the phenotype observed when spontaneous activity is disrupted in the retina. Whether and how neuronal activity regulates complement expression and function are open areas of investigation; however, on the basis of our data, we envision a model in which C1q is secreted locally from RGC terminals in an activity-dependent manner to regulate C3-CR3–dependent microglial synaptic phagocytosis (**Supplementary Fig. 5**).

Retinal C1q is required for retinogeniculate refinement

In the postnatal retinogeniculate system, both RGCs and microglia express C1q. Although microglia express more C1q than neurons (**Figs. 1c** and **2g**), several lines of evidence suggest that RGCs contribute appreciably to C1q levels and complement-dependent synaptic refinement in the postnatal dLGN. In retinal *Tgfbr2*$^{-/-}$ mice, which have reduced retinal C1q expression but normal microglial C1q expression, we observed defects in retinogeniculate refinement and microglial engulfment (**Figs. 6** and **7**), suggesting that microglial C1q expression cannot compensate functionally for the loss of RGC-derived C1q in complement-dependent synaptic refinement.

If RGC inputs are a critical source of C1q in the dLGN during synaptic refinement, how does C1q reach RGC terminals in the dLGN, far from the cell bodies in the retina? C1q is a large glycoprotein packaged and secreted by macrophages via traditional secretory pathways in the Golgi[25]. C1q then is secreted directly into the bloodstream by circulating macrophages. In RGCs, however, proteins that are produced and packaged in the soma in the retina have a long distance to travel to axon terminals in the dLGN. Given that in the retinal *Tgfbr2*$^{-/-}$ mice we observed reduced C1q levels compared to those in WT mice in the retina (**Fig. 4a–d**), the optic nerve (**Fig. 4e**,**f**) and the dLGN (**Fig. 5**), we hypothesize that C1q is transported along RGC axons to the dLGN in secretory vesicles, per its packaging and secretion

in macrophages. Alternatively, local translation and synthesis of C1q within RGC axons in the optic nerve or the dLGN is possible, although there have been no previous reports of local translation of C1q. Given the importance of spontaneous retinal activity in driving synaptic refinement and given that C1q regulation by TGF-β seems to be restricted to neurons (**Figs. 1c** and **4b**), we speculate that C1q secretion from RGC inputs may be regulated by neuronal activity and act as a molecular cue linking information about the retina to the dLGN to drive proper circuit development.

TGF-β: regulating neuronal C1q and CNS development

In the immune system, TGF-β is characterized as an anti-inflammatory cytokine that dampens the immune response. In the mammalian nervous system, TGF-β signaling pathways regulate diverse developmental processes, including neuronal survival and programmed cell death, axon specification, and synaptogenesis. TGF-β signaling modulates embryonic and postnatal periods of programmed cell death in the mouse retina[26] and also amplifies the efficacy of neurotrophic factors critical for cell survival, such as glia-derived neurotrophic factor[27]. In the developing rodent neocortex, TGF-β signaling is necessary and sufficient for axon specification[28]. Recent work also has shown that TGF-β regulates synaptogenesis in cortical neurons *in vitro*[29] and at the *Drosophila melanogaster* and *Xenopus laevis* neuromuscular junctions (NMJs)[30]. At the *Drosophila* NMJ, glia produce ligands that are TGF-β family members[31], and they direct synaptogenesis by regulating a neuron-derived TGF-β family member and the downstream Rac guanine nucleotide exchange factor Trio[32]. Also in *Drosophila*, TGF-β directs large-scale neuronal and axonal remodeling during metamorphosis[33,34]. TGF-β also affects synaptic function at excitatory and inhibitory synapses in the pre-Bötzinger complex in the mouse brainstem[35] and modulates sensory neuron excitability and synaptic efficacy at sensorimotor synapses in the sea slug *Aplysia*[36].

In the present study, we found that TGF-β signaling in postnatal RGCs was required for developmental synaptic refinement. Given the many important roles of TGF-β in development, we characterized other aspects of retinal development and found no significant deficits in the retinal *Tgfbr2*$^{-/-}$ mouse. Disrupting TGFβRII in the retina did not dramatically affect the number of retinal neurons or retinal morphology. Moreover, despite the role for TGFβRII in axon specification in cortex, disruption of TGFβRII signaling in the retina did not alter axon specification in the retina or axon caliber in the optic nerve (**Supplementary Fig. 2f–h**), suggesting that other mechanisms underlie axon development and specification in RGCs. Although we have not quantified synapses in the dLGN of retinal *Tgfbr2*$^{-/-}$ mice, it is unlikely that defective synaptogenesis could explain our phenotype, as we observed an increase in overlap between eye-specific territories. Furthermore, previous studies have reported that TGF-β is not synaptogenic in RGC cultures[10], further supporting the idea that synaptogenesis is likely normal in these mice.

Together our data implicate TGF-β as a key regulator of synaptic refinement in the mammalian CNS. In *Drosophila*, a class of TGF-β family members together with an immunoglobulin superfamily member protein, Plum, has been implicated in the dramatic remodeling that occurs during metamorphosis in the CNS and at the NMJ[33,34]. This finding combined with our findings raises the question of whether TGF-β signaling represents an important signal for synaptic remodeling throughout the nervous system. Could TGF-β initiate a synaptic refinement gene program in RGCs or other neurons that undergo refinement? Interestingly, C1q and TGF-β expression are expressed in the auditory system in embryonic and postnatal spiral ganglion neurons[37] around the time when spiral ganglion cell inputs onto outer hair cells are refined[38]. Little is known about the synaptic refinement mechanisms in the auditory system; however, this developmental expression of C1q and TGF-β suggests that the same mechanism for synapse elimination may drive refinement in both the auditory and visual systems. In both of these systems, C1q expression in sensory neurons (RGCs and spiral ganglion neurons) is developmentally regulated and restricted to periods of developmental synaptic remodeling. These findings are consistent with our hypothesis that neuron-derived C1q is critical for synaptic refinement, although it remains unclear whether TGF-β regulates *C1q* or other refinement genes in other brain regions.

Implications of TGF-β regulation of C1q in disease

Our findings also have important implications for understanding the mechanisms underlying synapse elimination in the diseased brain. Dysregulation of immune system components, including complement proteins and cytokines, has been demonstrated in many CNS disorders, including epilepsy, schizophrenia and neurodegenerative diseases such as glaucoma and Alzheimer's disease. In particular, TGF-β localizes to β-amyloid plaques and has been linked to the formation of these plaques in Alzheimer's disease[39], and blocking TGF-β and Smad2/3 signaling mitigates plaque formation in Alzheimer's mouse models[40]. C1q associates with plaques in Alzheimer's brains as well[41], and in mouse models of Alzheimer's, C1q-deficiency has been shown to be neuroprotective[42]. Synapse loss and/or dysfunction have emerged as early hallmarks of neurodegenerative diseases, suggesting that aberrant complement upregulation may reactivate the developmental synapse elimination pathway in disease to promote synapse loss. Our work demonstrating a new link between TGF-β signaling, complement and synapse elimination opens new avenues of investigation into the role of this regulatory mechanism for C1q in these disorders and in other regions of the healthy CNS during development.

METHODS

Methods and any associated references are available in the online version of the paper.

Note: Any Supplementary Information and Source Data files are available in the online version of the paper.

ACKNOWLEDGMENTS

We thank C. Chen, L. Benowitz, D.P. Schafer and M. Buckwalter for comments on the manuscript and critical discussion. In addition we thank A. Stephan, B. Barres and A. Tenner for assistance with anti-C1q antibody production and characterization. We also thank M. Rasband (Baylor College of Medicine) for the βIV spectrin antibody. Thank you to D.P. Schafer and E.K. Lehrman for technical expertise on the microglial engulfment assay and Imaris image analysis, T. Nelson for technical assistance, and the imaging core at Boston Children's Hospital, including T. Hill, for technical support. This work was supported by grants from the Smith Family Foundation (B.S.), Dana Foundation (B.S.), Ellison Foundation (B.S.), John Merck Scholars Program (B.S.), NINDS (RO1-NS-07100801; B.S.), NIDA (RO1-DA-15043; B.A. Barres) and NIH (P30-HD-18655; MRDDRC Imaging Core).

AUTHOR CONTRIBUTIONS

A.R.B. conducted all experiments, performed data analysis and wrote the manuscript. B.S. advised on and supervised the project and co-wrote the manuscript.

COMPETING FINANCIAL INTERESTS

The authors declare no competing financial interests.

1. Huh, G.S. *et al.* Functional requirement for class I MHC in CNS development and plasticity. *Science* **290**, 2155–2159 (2000).
2. Bjartmar, L. *et al.* Neuronal pentraxins mediate synaptic refinement in the developing visual system. *J. Neurosci.* **26**, 6269–6281 (2006).
3. Stevens, B. *et al.* The classical complement cascade mediates CNS synapse elimination. *Cell* **131**, 1164–1178 (2007).
4. Campbell, G. & Shatz, C.J. Synapses formed by identified retinogeniculate axons during the segregation of eye input. *J. Neurosci.* **12**, 1847–1858 (1992).
5. Sretavan, D. & Shatz, C.J. Prenatal development of individual retinogeniculate axons during the period of segregation. *Nature* **308**, 845–848 (1984).
6. Hooks, B.M. & Chen, C. Distinct roles for spontaneous and visual activity in remodeling of the retinogeniculate synapse. *Neuron* **52**, 281–291 (2006).
7. Schafer, D.P. *et al.* Microglia sculpt postnatal neural circuits in an activity and complement-dependent manner. *Neuron* **74**, 691–705 (2012).
8. Boulanger, L.M. Immune proteins in brain development and synaptic plasticity. *Neuron* **64**, 93–109 (2009).
9. Ullian, E.M., Sapperstein, S.K., Christopherson, K.S. & Barres, B.A. Control of synapse number by glia. *Science* **291**, 657–661 (2001).
10. Christopherson, K.S. *et al.* Thrombospondins are astrocyte-secreted proteins that promote CNS synaptogenesis. *Cell* **120**, 421–433 (2005).
11. Allen, N.J. *et al.* Astrocyte glypicans 4 and 6 promote formation of excitatory synapses via GluA1 AMPA receptors. *Nature* **486**, 410–414 (2012).
12. Foo, L.C. *et al.* Development of a method for the purification and culture of rodent astrocytes. *Neuron* **71**, 799–811 (2011).
13. Ullian, E.M., Christopherson, K.S. & Barres, B.A. Role for glia in synaptogenesis. *Glia* **47**, 209–216 (2004).
14. Stephan, A.H. *et al.* A dramatic increase of C1q protein in the CNS during normal aging. *J. Neurosci.* **33**, 13460–13474 (2013).
15. Massagué, J. How cells read TGF-β signals. *Nat. Rev. Mol. Cell Biol.* **1**, 169–178 (2000).
16. Inman, G.J. *et al.* SB-431542 is a potent and specific inhibitor of transforming growth factor-β superfamily type I activin receptor-like kinase (ALK) receptors ALK4, ALK5, and ALK7. *Mol. Pharmacol.* **62**, 65–74 (2002).
17. de Melo, J., Qiu, X., Du, G., Cristante, L. & Eisenstat, D.D. Dlx1, Dlx2, Pax6, Brn3b, and Chx10 homeobox gene expression defines the retinal ganglion and inner nuclear layers of the developing and adult mouse retina. *J. Comp. Neurol.* **461**, 187–204 (2003).
18. Rowan, S. & Cepko, C.L. Genetic analysis of the homeodomain transcription factor Chx10 in the retina using a novel multifunctional BAC transgenic mouse reporter. *Dev. Biol.* **271**, 388–402 (2004).
19. Barres, B.A., Silverstein, B.E., Corey, D.R. & Chun, L.L.Y. Immunological, morphological, and electrophysiological variation among retinal ganglion cells purified by panning. *Neuron* **1**, 791–803 (1988).
20. Torborg, C.L. & Feller, M.B. Unbiased analysis of bulk axonal segregation patterns. *J. Neurosci. Methods* **135**, 17–26 (2004).
21. Schafer, D.P., Lehrman, E.K. & Stevens, B. The "quad-partite" synapse: Microglia-synapse interactions in the developing and mature CNS. *Glia* **61**, 24–36 (2012).
22. Tremblay, M.E. *et al.* The role of microglia in the healthy brain. *J. Neurosci.* **31**, 16064–16069 (2011).
23. Corriveau, R.A., Huh, G.S. & Shatz, C.J. Regulation of class I MHC gene expression in the developing and mature CNS by neural activity. *Neuron* **21**, 505–520 (1998).
24. Tsui, C.C. *et al.* Narp, a novel member of the pentraxin family, promotes neurite outgrowth and is dynamically regulated by neuronal activity. *J. Neurosci.* **16**, 2463–2478 (1996).
25. Yuzaki, M. Synapse formation and maintenance by C1q family proteins: a new class of secreted synapse organizers. *Eur. J. Neurosci.* **32**, 191–197 (2010).
26. Beier, M., Franke, A., Paunel-Görgülü, A.N., Scheerer, N. & Dünker, N. Transforming growth factor beta mediates apoptosis in the ganglion cell layer during all programmed cell death periods of the developing murine retina. *Neurosci. Res.* **56**, 193–203 (2006).
27. Peterziel, H., Unsicker, K. & Krieglstein, K. TGFβ induces GDNF responsiveness in neurons by recruitment of GFRα1 to the plasma membrane. *J. Cell Biol.* **159**, 157–167 (2002).
28. Yi, J.J., Barnes, A.P., Hand, R., Polleux, F. & Ehlers, M.D. TGF-[beta] Signaling Specifies Axons during Brain Development. *Cell* **142**, 144–157 (2010).
29. Diniz, L.P. *et al.* Astrocyte-induced synaptogenesis is mediated by transforming growth factor β signaling through modulation of d-serine levels in cerebral cortex neurons. *J. Biol. Chem.* **287**, 41432–41445 (2012).
30. Feng, Z. & Ko, C.-P. Schwann cells promote synaptogenesis at the neuromuscular junction via transforming growth factor-β1. *J. Neurosci.* **28**, 9599–9609 (2008).
31. Fuentes-Medel, Y. *et al.* Integration of a retrograde signal during synapse formation by glia-secreted TGF-β ligand. *Curr. Biol.* **22**, 1831–1838 (2012).
32. Ball, R.W. *et al.* Retrograde BMP signaling controls synaptic growth at the NMJ by regulating trio expression in motor neurons. *Neuron* **66**, 536–549 (2010).
33. Awasaki, T., Huang, Y., O'Connor, M.B. & Lee, T. Glia instruct developmental neuronal remodeling through TGF-β signaling. *Nat. Neurosci.* **14**, 821–823 (2011).
34. Yu, X.M. *et al.* Plum, an immunoglobulin superfamily protein, regulates axon pruning by facilitating TGF-β signaling. *Neuron* **78**, 456–468 (2013).
35. Heupel, K. *et al.* Loss of transforming growth factor-beta 2 leads to impairment of central synapse function. *Neural Dev.* **3**, 25 (2008).
36. Chin, J., Angers, A., Cleary, L.J., Eskin, A. & Byrne, J.H. Transforming growth factor beta 1 alters synapsin distribution and modulates synaptic depression in *Aplysia*. *J. Neurosci.* **22**, RC220 (2002).
37. Lu, C.C., Appler, J.M., Houseman, E.A. & Goodrich, L.V. Developmental profiling of spiral ganglion neurons reveals insights into auditory circuit assembly. *J. Neurosci.* **31**, 10903–10918 (2011).
38. Huang, L.-C., Thorne, P.R., Housley, G.D. & Montgomery, J.M. Spatiotemporal definition of neurite outgrowth, refinement and retraction in the developing mouse cochlea. *Development* **134**, 2925–2933 (2007).
39. Wyss-Coray, T. *et al.* Amyloidogenic role of cytokine TGF-β1 in transgenic mice and in Alzheimer's disease. *Nature* **389**, 603–606 (1997).
40. Town, T. *et al.* Blocking TGF-β–Smad2/3 innate immune signaling mitigates Alzheimer-like pathology. *Nat. Med.* **14**, 681–687 (2008).
41. Afagh, A., Cummings, B.J., Cribbs, D.H., Cotman, C.W. & Tenner, A.J. Localization and cell association of C1q in Alzheimer's disease brain. *Exp. Neurol.* **138**, 22–32 (1996).
42. Fonseca, M.I., Zhou, J., Botto, M. & Tenner, A.J. Absence of C1q leads to less neuropathology in transgenic mouse models of Alzheimer's disease. *J. Neurosci.* **24**, 6457–6465 (2004).
43. McCarthy, K.D. & De Vellis, J. Preparation of separate astroglial and oligodendroglial cell cultures from rat cerebral tissue. *J. Cell Biol.* **85**, 890–902 (1980).

ONLINE METHODS

Mice and rats. Floxed TGFβRII mice (B6.129S6-*Tgfbr2*^{tm1Hlm}) were obtained from the NCI Mouse Repository and crossed to the *CHX10-cre* line, Tg(Chx10-EGFP/cre,-ALPP)2Clc/J (Jackson Lab), to generate retina-specific *Tgfbr2*$^{-/-}$ mice. *C1qa*$^{-/-}$ mice (C57BL/6 background) were generously provided by M. Botto[44]. Experiments were approved by the Boston Children's Hospital institutional animal use and care committee in accordance with NIH guidelines for the humane treatment of animals. Both male and females were included in the study. Total mice used for all experiments was approximately 300. Rats were obtained from Charles River Laboratories. Sprague-Dawley rats were used for all tissue culture experiments. Total rats used was approximately 80 litters (ten P8 rats per litter).

Neuron and astrocyte cultures. Retinal ganglion cells were cultured from P8 Sprague-Dawley rats after serial immunopanning steps to yield >99.5% purity as described[19]. Cells were maintained in serum-free medium as described[45]. Cortical astrocytes were prepared from P1–P2 rat cortices as previously described[9]. Retinal astrocytes were prepared from P8 mouse or Sprague-Dawley rat retinas by adapting described methods for purification of cortical astrocytes[12]. After first immunopanning away microglia and RGCs, an anti-ITGB5-coated Petri plate was used to isolate astrocytes from remaining cells in suspension. Purified cortical astrocytes were prepared as described[12]. Purified retinal and cortical astrocytes were maintained in a defined serum-free medium supplemented with hbEGF as described[12]. Astrocyte conditioned medium (ACM) was prepared as previously described[9]. Astrocytes were switched to minimal medium (Neurobasal plus glutamine, penicillin and streptomycin, and sodium pyruvate) once confluent. Medium was collected after 5 d and concentrated tenfold using Vivaspin columns (Sartorius).

qPCR. RGCs, microglia and astrocytes were acutely isolated using immunopanning as described above from either mice or rats at indicated ages. For acute isolation experiments, RNA was collected directly from the immunopanning plate without culturing the cells. For cultured RGC experiments, total RNA was prepared, cDNA was synthesized, and qPCR performed using the Applied Biosystems Cells to Ct Power SYBR Green kit as described by the manufacturer. Briefly, cell lysates were collected from 80,000 RGCs in provided lysis buffer and cDNA was synthesized directly from this lysate. qPCR reactions were assembled for the genes of interest (*C1qa*, *C1qb*, Klf10 (*Tieg*), *Gapdh*) using 4 µl of cDNA per reaction and samples were run on the Rotogene qPCR machine (Qiagen). Expression levels were compared using the ddC_t method normalized to *Gapdh*.

Immunohistochemistry. Brains and eyes were collected from mice after transcardial perfusion with 4% paraformaldehyde (PFA). Tissue was then immersed in 4% PFA for 2 h following perfusion, cryoprotected in 30% sucrose and embedded in a 2:1 mixture of OCT and 20% sucrose PBS. Tissue was cryosectioned (12–14 µm) and sections were dried, washed three times in PBS and blocked with 2% BSA plus 0.2% Triton X in PBS for 1 h. Primary antibodies were diluted in antibody buffer (plus 0.05% Triton and 0.5% BSA) as follows: C1q (Epitomics, custom antibody synthesis, undiluted culture supernatant, validated in ref. 14), C3 (Cappel, cat. no. 855730, 1:300, validated in ref. 3), vglut2 (Millipore, cat. no. AB2251,1:2,000, validated in ref. 7), TGFβRII (R&D Systems, cat. no. AF-241-NA, 1:200, validated in **Fig. 3d** and in ref. 28), pSmad (Millipore, cat. no. AB3849, 1:200, validated in ref. 46), calretinin (Millipore, cat. no. MAB1568, 1:1,000, validated in ref. 47), Iba1 (Wako, cat. no. 019-19741, 1:400, validated in ref. 7), CD68 (Serotec, cat. no. MCA1957, 1:300, validated in ref. 7) and TUJ1 (Covance, cat. no. MMS-435P, 1:400, validated in ref. 7). Samples were incubated overnight at 4 °C. Secondary Alexa-conjugated antibodies (donkey anti-rabbit 488, Invitrogen cat. no. A21206; donkey anti-goat 488, Invitrogen cat. no. A11055; donkey anti–guinea pig Alexa 594, Jackson cat. no. 706-585-148; donkey anti-mouse 594, Invitrogen cat. no. A21203; donkey anti-rat 488, Invitrogen cat. no. A21208) were added at 1:200 in antibody buffer for 2 h at room temperature. Slides were mounted in Vectashield (plus DAPI) and imaged using a Zeiss Axiocam and Zeiss LSM700 or a PerkinElmer Ultraview Vox spinning disk confocal microscope.

ELISA. The 7-plex Mouse Inflammatory Cytokine kit (MSD, Cat. # K15012C-1, validated in ref. 48) was used to profile cytokines in ACM. Freshly prepared ACM was profiled according to the manufacturer's provided protocol. Standards were diluted in minimal medium used to make ACM for greater accuracy. Plates were read and data were acquired and analyzed using the MSD Sector Imager 2400. ELISA kits were obtained for TGF-β1, TGF-β2 and TGF-β3 separately (R&D Systems: TGF-β1, cat. no. DB100B, validated in ref. 51; TGF-β2, cat. no. DB250, validated in ref. 49; TGF-β3, cat. no. DY243, validated in ref. 50) and were performed according to manufacturer's instructions.

Western blot. RGC and whole retina lysates were collected and homogenized in RIPA buffer with complete protease inhibitors (Roche). Samples were boiled for 5 min in SDS sample buffer, resolved by SDS PAGE, transferred to PVDF membranes and immunoblotted. Antibodies were diluted in 5% milk in PBS plus 0.1% Tween. Antibodies were rabbit anti-C1qA polyclonal (Epitomics, custom antibody, 1:5,000, specificity validated in ref. 14) and goat anti-TGFβRII (R&D Systems, cat. no. AF-241-NA, 1:1,000, validated in refs. 26 and 28). Secondary antibodies were diluted 1:10,000 in 5% milk in PBS plus 0.1% Tween (donkey anti-rabbit, Jackson cat. no. 712-035-152; rabbit anti-goat, Zymed cat. no. 81-1620).

***In situ* hybridization.** *In situ* hybridization for C1qb was performed on 12-µm retinal sections as previously described[3]. Probes targeting the entire *C1qb* coding sequence (Open Biosystems clone 5715633) were generated by digesting the plasmid with EcoRI and performing *in vitro* transcription with T7 polymerase using the DIG RNA labeling kit (Roche Applied Science) as per the manufacturer's instructions. 1.8-kb probes were then cleaved to form 300-bp probes by alkaline hydrolysis before use.

LGN analysis. Mice received intraocular injection of cholera toxin-β subunit (CTB) and were sacrificed the following day. Tissue was processed and analyzed as previously described[3,51]. Mouse pups were anesthetized with inhalant isoflurane. Mice received intravitreal injections of cholera toxin-β subunit (CTB) conjugated to Alexa 488 (green label) in the left eye and intravitreal injection of CTB conjugated to Alexa 594 (red label) in the right eye as described[2]. Images were digitally acquired using the Zeiss Axiocam. All images were collected and quantified blind to experimental conditions and compared to age-matched littermate controls. Gains and exposures were established for each label. Raw images of the dLGN were imported to Photoshop (Adobe), and the degree of left and right eye axon overlap in dLGN was quantified using a multi-threshold protocol as previously described[2] and using threshold-independent *R*-value analysis as described[20]. For threshold independent analysis, we performed background subtraction using a 200-pixel rolling ball radius filter and normalized the images. We then calculated the *R* value ($\log(F_{ipsi}/F_{contra})$) for each pixel and determined the variance of the *R*-value distribution for each image (four images per animal). Pseudocolored images representing the *R*-value distribution were generated in ImageJ.

Retinal cell counts. Retinal flat mounts were prepared by dissecting out retinas whole from the eyecup and placing four relieving cuts along the major axes, radial to the optic nerve. Each retina was stained with DAPI (Vector Laboratories, Burlingame, CA) to reveal cell nuclei. Measurements of total cell density in the ganglion cell layer (which includes both ganglion cells and displaced amacrine cells) were carried out blind to genotype from matched locations in the central and peripheral retina for all four quadrants of each retina. Quantification was limited to P30 retinas, which is an age subsequent to ganglion cell genesis and apoptosis in the mouse. For each retina (1 retina per animal; $n = 3$ mice per treatment condition or genotype), 12 images of peripheral retina and 8 images of central retina were collected. For each field of view collected (20 per retina), Macbiophotonics ImageJ software (NIH) was used to quantify the total number of DAPI-stained nuclei using the nuclei counter plugin and TUJ1-positive cells were counted using the cell counter plugin. All analyses were performed blind to genotype or drug treatment.

***z*-stack image and microglial engulfment analysis.** *In vivo* microglia phagocytosis assay and analyses were performed as previously described in detail in ref. 7. In brief, mice received intraocular injections of anterograde tracers at P4. All mice were sacrificed at P5 and brains were fixed in 4% PFA overnight at 4 °C. Only those brains with sufficient dye fills were analyzed. For each animal, two sections of medial dLGN were chosen for imaging for reconstruction of RGC inputs and C1q staining, as well as for microglia engulfment analysis. Images were acquired on a spinning disc confocal at 60× magnification using 0.2 µm *z*-steps. For each dLGN, 4–8 fields were imaged in the ipsilateral territory and

4–8 fields were imaged in the contralateral territory (minimum of 8 fields per dLGN, 16 fields per animal). Subsequent images were processed and quantified using ImageJ (NIH) and Imaris software (Bitplane). For subsequent acquired *z*-stacks, ImageJ (NIH) was used to subtract background from all fluorescence channels (rolling ball radius = 10) and a mean filter was used for the EGFP channel (stained for Iba1) of 1.5. Subsequently, Imaris software (Bitplane) was used to create 3D volume surface renderings of each *z*-stack. Surface rendered images were used to determine the volume of the microglia, all RGC inputs and the volume of C1q staining. To visualize and measure the volume of engulfed inputs, any fluorescence that was not within the microglia volume was subtracted from the image using the mask function. The remaining engulfed/internal fluorescence was surface rendered using parameters previously determined for all RGC inputs/C1q and total volume of engulfed/internal inputs was calculated. To determine percentage engulfment (or percentage C1q-positive terminals), the following calculation was used: volume of internalized RGC input (or volume of C1q)/volume microglial cell (or RGC inputs). For KO engulfment experiments, all analyses were performed blind.

Microglia density quantification. For quantification of cell density, dLGNs from two coronal sections were imaged for each animal (n = 3 per treatment condition or genotype). To capture the entire dLGN, a 10× field was acquired. Microglia were subsequently counted from each 10× field. To calculate the density of microglia, the area of the dLGN was measured using ImageJ software (NIH). All analyses were performed blind to genotype or drug treatment.

Quantification of microglial activation state. Activation state was quantified based on established methods described in ref. 7. Immunohistochemistry was performed on 40-µm cryosections with antibodies against Iba1 (Wako, rabbit anti-Iba1, cat. no. 019-19741, validated in ref. 7) and CD68 (Serotec, cat. no. MCA1957, validated in ref. 7). For each genotype, two 20× fields of view were analyzed on a spinning-disk confocal microscope using 2-µm *z*-steps. The activation state was then determined using a maximum intensity projection. Iba1 staining was used to assess morphology on the basis of the number of branches, and the expression pattern of CD68 was analyzed and scored as 0 (no or scarce expression), 1 (punctate expression) or 2 (aggregated expression or punctate expression all over the cell). Scores from 0 to 3 for number of branches or 0 to 2 were assigned on the basis of Iba1 and CD68 staining, and these scores were summed to give the most activated microglia an overall score of 5 and least activated a score of 0. For each genotype, four mice were analyzed and all analysis was performed blind.

Statistical analysis. For all statistical analyses, data distribution was assumed to be normal, but this was not formally tested. GraphPad Prism 5 software (La Jolla, CA) was used for all statistical tests. Analyses used include one-way ANOVA, two-way ANOVA and Student's *t*-test. For ANOVA analysis, Bonferroni *post hoc* tests were used. Igor was used to calculate the *R*-value variance in **Figure 6**. No statistical methods were used to predetermine sample sizes, but our sample sizes are similar to those reported in previous publications[3,7]. Data collection and analysis were performed blind to the conditions of the experiments. Also, data for each experiment were collected and processed randomly and animals were assigned to various experimental groups randomly as well. All n and P values and statistical tests are indicated in figure legends. All error bars represent s.e.m., and mean ± s.e.m. is plotted for all graphs except where noted.

44. Botto, M. *et al.* Homozygous C1q deficiency causes glomerulonephritis associated with multiple apoptotic bodies. *Nat. Genet.* **19**, 56–59 (1998).
45. Meyer-Franke, A., Kaplan, M.R., Pfrieger, F.W. & Barres, B.A. Characterization of the signaling interactions that promote the survival and growth of developing retinal ganglion cells in culture. *Neuron* **15**, 805–819 (1995).
46. Doyle, K. *et al.* TGFβ signaling in the brain increases with aging and signals to astrocytes and innate immune cells in the weeks after stroke. *J. Neuroinflam.* **7**, 62 (2010).
47. Dyer, M.A. & Cepko, C.L. p57 (Kip2) regulates progenitor cell proliferation and amacrine interneuron development in the mouse retina. *Development* **127**, 3593–3605 (2000).
48. Lázár-Molnár, E. *et al.* Programmed death-1 (PD-1)–deficient mice are extraordinarily sensitive to tuberculosis. *Proc. Natl. Acad. Sci. USA* **107**, 13402–13407 (2010).
49. Truckenmiller, M.E. *et al.* AF5, a CNS cell line immortalized with an N-terminal fragment of SV40 large T: growth, differentiation, genetic stability, and gene expression. *Exp. Neurol.* **175**, 318–337 (2002).
50. Liu, G. *et al.* Requirement of Smad3 and CREB-1 in Mediating Transforming Growth Factor-β (TGFβ) Induction of TGFβ3 Secretion. *J. Biol. Chem.* **281**, 29479–29490 (2006).
51. Jaubert-Miazza, L. *et al.* Structural and functional composition of the developing retinogeniculate pathway in the mouse. *Vis. Neurosci.* **22**, 661–676 (2005).

doi:10.1038/nn.3560